www.sciencemag.org/cgi/content/full/1167324/DC1

Supporting Online Material for

Auxin-Dependent Patterning and Gamete Specification in the *Arabidopsis* Female Gametophyte

Gabriela C. Pagnussat, Monica Alandete-Saez, John L. Bowman, Venkatesan Sundaresan*

*To whom correspondence should be addressed. E-mail: sundar@ucdavis.edu

Published 4 June 2009 on *Science* Express
DOI: 10.1126/science.1167324

This PDF file includes:

Supporting Online Material

Materials and methods

Plant growth conditions

Seeds were sterilized in 20% (v/v) sodium-hypochlorite, washed with sterile water and plated on MS medium (Sigma-Aldrich). Seedlings were then transferred onto soil and grown in a growth chamber with a 16-hlight/ 8-h-dark cycle at 22°C with 60% relative humidity. For crosses, flowers of the female parent were manually emasculated 2 days before anthesis and cross-pollinated 2 days later.

Histology and microscopy

To prepare cleared whole-mount preparations, pistils containing at least 20 ovules were dissected and cleared overnight in Hoyers solution (*S1*). The dissected pistils were observed on a Zeiss Axioplan imaging 2 microscope (Zeiss, Oberkochem, Germany) under DIC optics. Images were captured on an Axiocam HRC CCD camera (Zeiss) with the Axiovision program (version 3.1, Zeiss). For GUS staining, developing carpels and siliques were dissected and incubated in GUS staining buffer, as described (*S2*). Individual ovules were dissected from the pistils/siliques and cleared overnight with Hoyers solution (*S1*). The ovules were observed under DIC optics. For pollen tube growth pattern analysis, aniline blue staining was performed, as described (*S3*).

Constructs and Plant Transformation

The synthetic a*miR-ARFa* gene was designed with *miR164b* of *Arabidopsis* as a backbone (*S3*), targeting a sequence largely conserved between ARF1-8 and ARF19 (ELWHACA = GAGCTATGGCACGCTTGTGCA, Fig. S6). The synthetic miRNA was constructed by GenScript (Piscataway, New Jersey, USA). amiR-ARFa was excised from pUC57, cloned into 6OpTATA BJ36 (*S2*) and subsequently into the binary vector pMLBART (Op::amiR-ARFa BART). Op:amiR-ARFa BART was initially transformed into pAP3:LhG4 driver lines (*S4*) and individuals lacking petals and stamen development were selected for crossing with pES1:LhG4. 10op::*YUC1* was constructed by inserting *YUC1* cDNA (provided by Dr. Y. Zhao) behind an *OP* array (10OP-TATA-BJ36) (*S2*) and subsequently subcloned into the binary vector pCAMBIA 1300 (*CAMBIA*, Canberra, Australia). The plasmid was introduced into *Agrobacterium tumefaciens* strain GV3101 by electroporation and *Ler* wild-type plants were transformed with the floral dip method (*S5*).

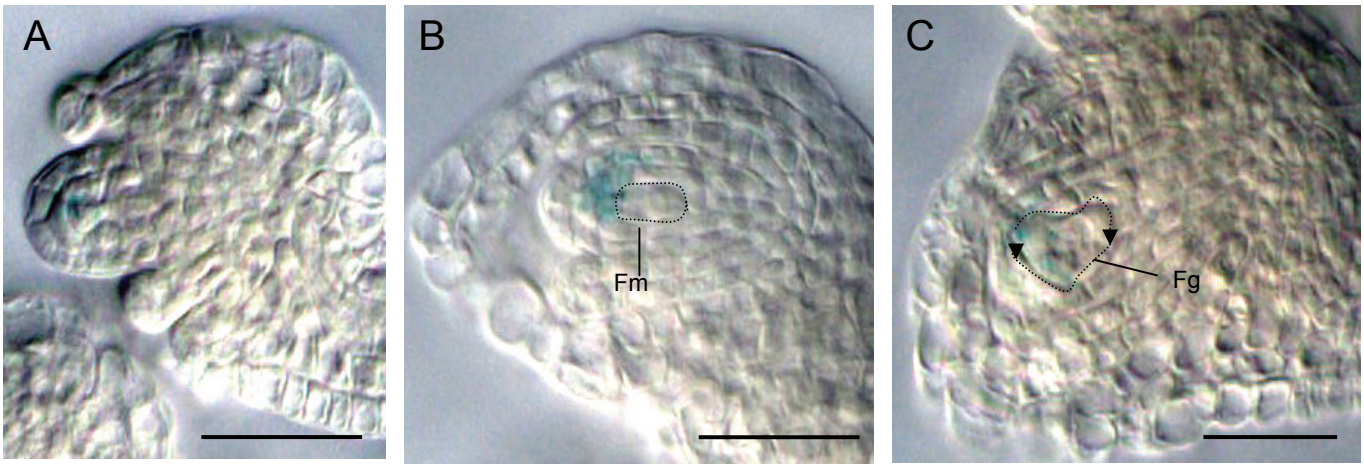

Fig. S1: Expression of the synthetic reporter *DR5::GUS* during female gametophyte development (A) Auxin signaling output could be detected during megasporogenesis at the distal tip of the nucellus. (B) At FG1 the signal is strongly detected in the nucellus, outside the embryo sac. (C) At FG3 stage the signal is detectable inside the embryo sac, at the micropylar pole. Arrowheads indicate the position of nuclei at FG3. Fm, functional megaspore; Fg, female gametophyte.

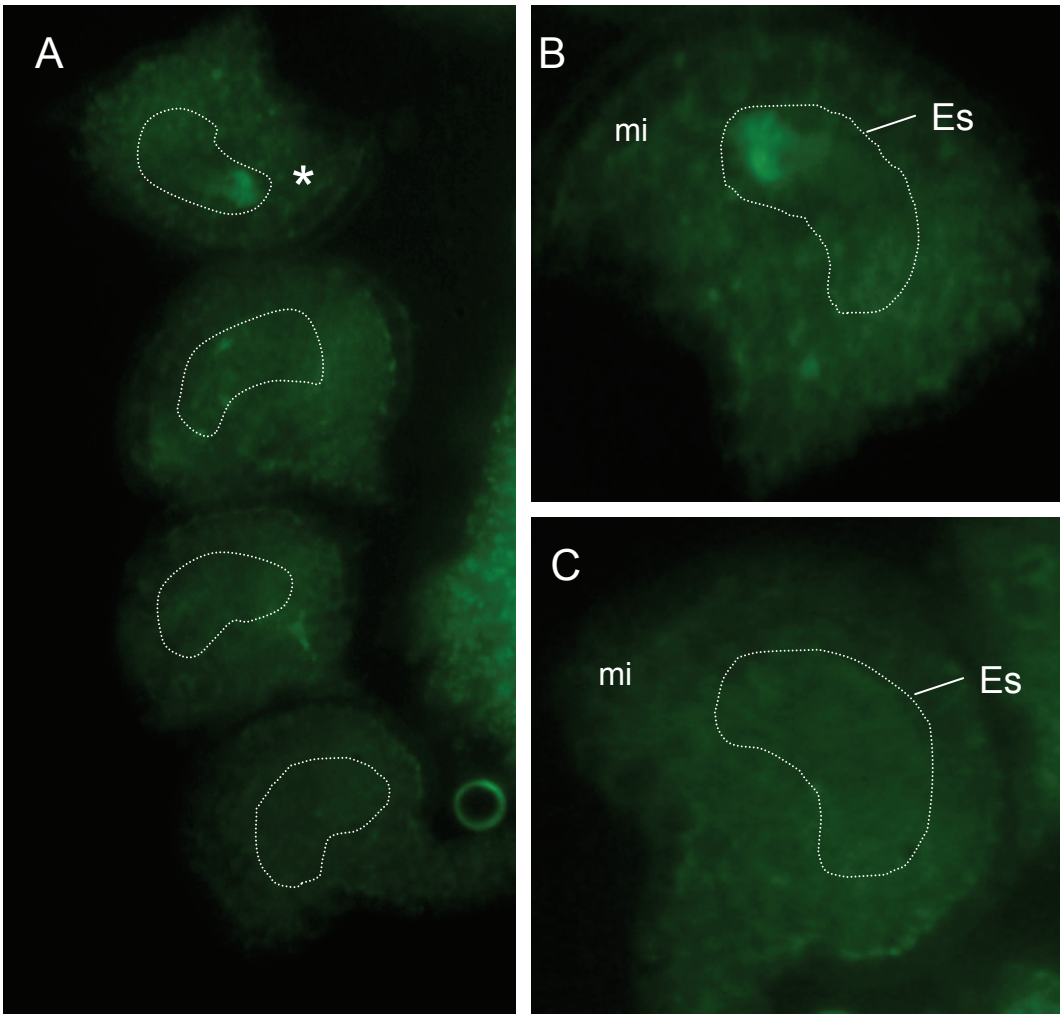

Fig. S2: Auxin signaling output is downregulated in pES1>>*amiR-ARFa* embryo sacs. (A) A pistils of a *pES1::LhG4/+; Op::amiR-ARFa/+; DRF::GFP/+* plant showing segregation for GFP expression in embryo sacs. Asterisk indicates embryo sac exhibiting the characteristic expression of the synthetic reporter *DR5::GFP*. (B) *GFP* expression is detected in one of the embryo sacs from a *pES1::LhG4/+; Op::amiR-ARFa/+; DRF::GFP/+* pistil. (C) An embryo sac showing no expression of the auxin reporter *DR5::GFP*. Embryo sacs are outlined by a dotted line. Es, embryo sac; mi, micropyle. Detailed results and quantification are shown in Table S1.

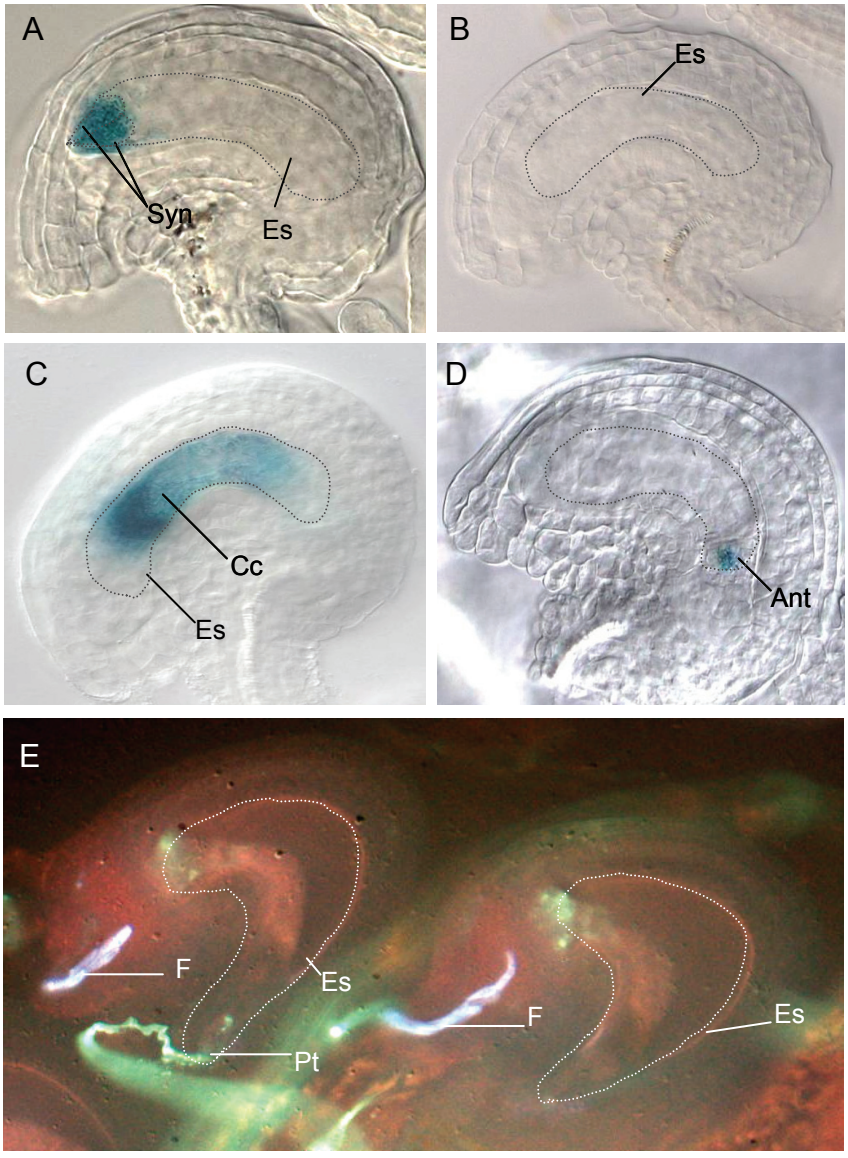

Fig. S3: Cell identities and pollen tube attraction in embryo sacs downregulated for ARF expression with *amiR-ARFa* driven by pES1 promoter. (A) two micropylar cells were GUS positive when the expression of a synergid-specific marker was tested in WT embryo sacs. (B) expression of the synergid-specific marker was never detected in ARF-downregulated embryo sacs. (C) Expression of a central cell marker in ARF-downregulated embryo sac was similar to WT. (D) Expression of an antipodal marker was similar to WT (S6). (E) Ovules showing segregation for WT embryo sac attracting a pollen tube on the left, and an ARF-downregulated embryo sac with loss of pollen tube attraction on the right. Ant, antipodal cells; Cc, central cell; Es, embryo sac; F, funiculus; Pt, pollen tube Syn, synergids.

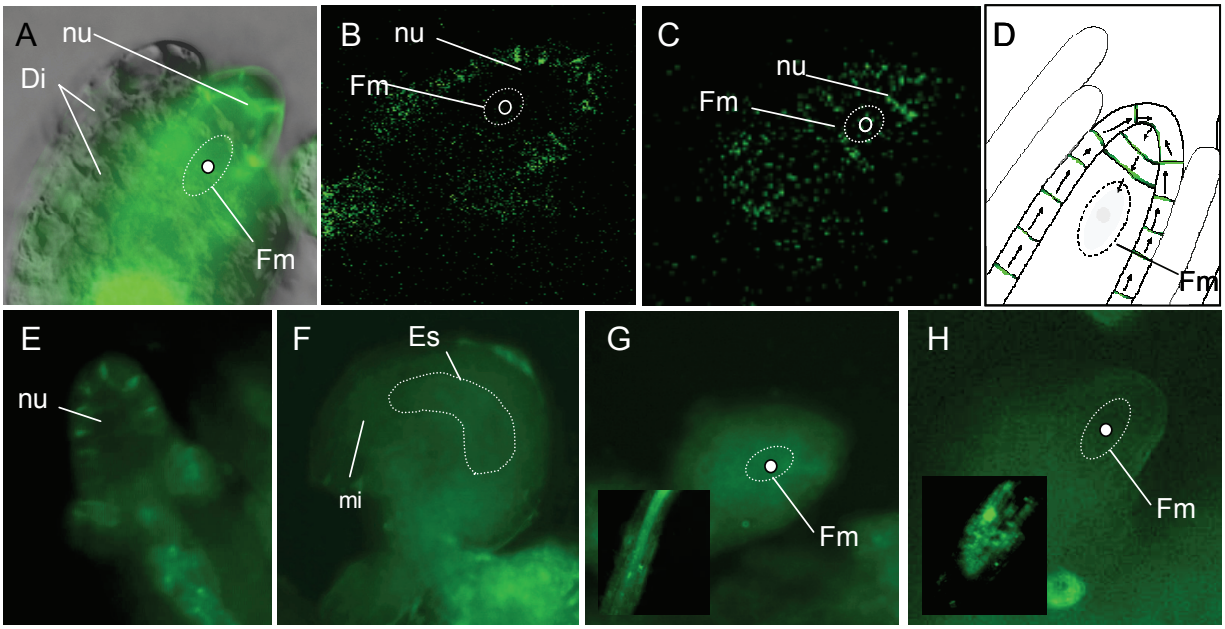

Fig. S4: *PIN* expression in the developing ovule. PIN1 was detected by following the localization of the reporter gene GFP in transgenic plants carrying a *PIN1::GFP* translational fusion (gift of J. Friml) (A) Epifluorescence image showing *PIN1* expression in the nucellus at FG1 stage. (B) Confocal image showing *PIN1* localization in the external layer of nucellar cells. (C) Confocal image showing *PIN1* expression in internal cells of the nucellus. (D) *PIN1* localization suggests that auxin flux in the nucellus might be involved in establishing an auxin maximum at FG1 stage. Green lines in the diagram indicate *PIN 1* localization. (E) Epifluorescence image showing *PIN1* expression in the nucellus at sporogenesis, prior to FG1 stage. (F) No *PIN1* expression could be detected in the nucellus or embryo sac after FG1 stage. Picture shows an ovule at FG6 stage in which only auto fluorescence is visible. (G) Epifluorescence image from *PIN3::GFP* transgenic plant showing no *PIN3* expression in the nucellus at FG1 stage. Inset, *PIN3* expression in the root is shown as a positive control for GFP activity. (H) Epifluorescence image from *PIN4::GFP* transgenic plant showing no *PIN4* expression in the nucellus at FG1 stage. Inset, *PIN4* expression in the root is shown as a positive control for GFP activity. Di, developing integuments; Es, embryo sac; Fm, indicates position of the functional megaspore; mi, indicates position of micropyle; nu, nucellus.

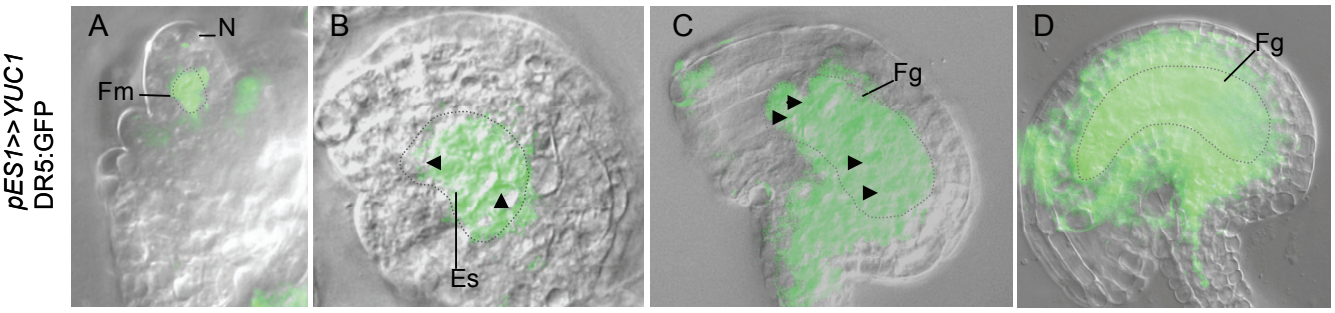

Fig. S5: *DR5::GFP* activity was detected in *pES1>>YUC1* female gametophytes from stages FG1 to FG6. (A) DR5 activity at FG1. (B) DR5 activity at FG3. (C) DR5 activity at FG4. (D) DR5 activity at FG6 (embryo sac after cellularization). Low activity was detected at the nucellus at FG1 (A). As a strong activity was detected inside the developing embryo sac, the exposure used was not enough to reveal the nucellar GFP. Arrowheads indicate positions of nuclei inside the embryo sac. Fm, functional megaspore; Fg, female gametophyte; N, nucellus; Es embryo sac

A

CTCGAGGAGAATGATGAAGGTGTGTGATGAGCAAGATGCACAAGCGTGCCATAGCTCTTACTAGCTCATATATACACTCTCACCACAAATG
CGTGTATATATGCGGAATTTTGTGATATAGATGTGTGTGTGTTGAGTGTGATGATATGGATGAGTTAGTTCGCGCTATGGCAATCTTGA
GCATCATGACCACTCCACCTTGGTGACGATGACGACGAGGGTTCAAGTGTTACGCACGTGGGAATATACTTATATCGATAAACACACACGT
GCGGGATCC

B

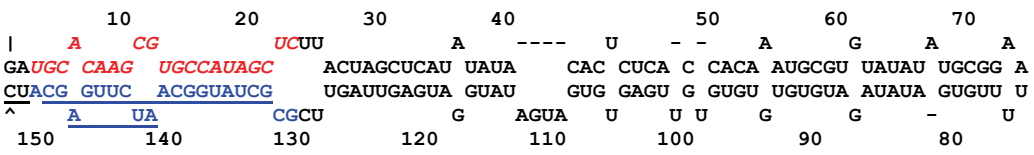

C

position	221111111111
in miR 3'	10987654321098765432 1 5'
rc amiR-ARFa	GAGCUAUGGCACGCUUGUGCA
ARF5/MP	GAGCUAUGGCACGCUUGUGCA
ARF7/NPH4	GAGCUAUGGCACGCUUGUGCU
ARF2	GAGCUAUGGCACGCUUGUGCU
ARF19	CAACUAUGGCACGCUUGUGCA
ARF8	GAGCUAUGGCAUGCUUGUGCU
ARF6	GAGCUCUGGCAUGCUUGUGCU
ARF3/ETTIN	GAGCUGUGGCAUGCUUGUGCU
ARF4	GAGCUUUGGCAUGCUUGUGCU
ARF1	GAGCUCUGGCAUGCCUGUGCU

D

Fig. S6: Design of the synthetic *amiR-ARFa* gene. (A) *miR164b* of *Arabidopsis* was used as a backbone, targeting a sequence largely conserved between ARF1-8 and ARF19 (ELWHACA = GAGCTATGGCACGCTTGTGCA). These ARFs belong to the MP, ETT and ARF1 clades, sometimes also referred to as the Class IIa, IIb and Ia ARFs (S7-S9). (B) predicted stem-loop. *italic* = *amiR-ARFa*. (C) Alignment of the reverse complement of the *amiR-ARFa* sequence with potential *ARF* targets in *Arabidopsis*. Mismatches are shown in red. On the basis of the effect of mismatches on cleavage of the *PHABULOSA* gene (S10), the first 4 genes are very likely to be targeted by the a-miRNA, with the remaining 5 genes in descending order are potential targets for cleavage or translational repression (S8 and S9). (D) Flower from a plant with down-regulated ARF expression in floral organ primordia. When *amiR-ARFa* is driven in the second and third whorls of the flower with the *APETALA3* (*AP3*) promoter (*pAP3>>amiR-ARFa*), there was a loss of lateral organs in these whorls, a result consistent with *amiR-ARFa* targeting *ARF5/MONOPTEROS* (S11). Lines with strong phenotypes lacked both petals and stamens, whereas weaker phenotype lines lacked only petals as shown in this image (two sepals have been removed).

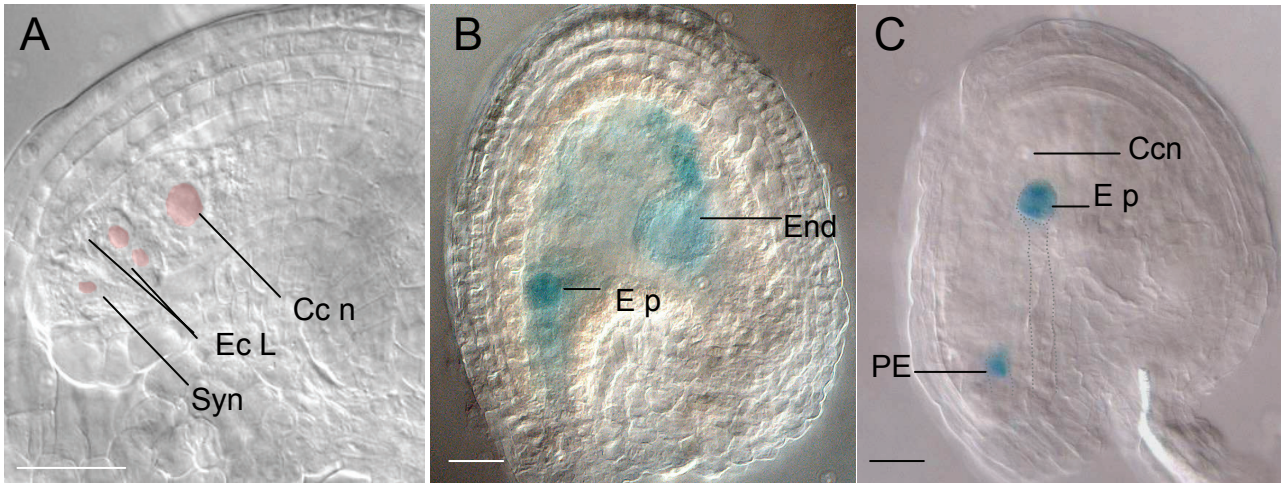

Fig. S7: Cell identity is altered in *tir1 afb1-1 afb2-2 afb3-3* quadruple mutant embryo sacs. (A) Phenotype of an embryo sac from a *tir1 afb1-1 afb2-2 afb3-3* quadruple mutant plant showing two egg cell-like cells and only one synergid cell. (B and C), GUS expression patterns detected after pollinating a *tir1 afb1-1 afb2-2 afb3-3* quadruple mutant with pollen from transgenic plants carrying the *PFAC1IE:GFP-GUS:TFAC1* construct. *FAC1* (Embryonic Factor 1) encodes a putative AMP deaminase (EC:3.5.4.6) and is expressed in both the developing embryo and endosperm from the paternal allele (Xu et al., 2005). (B) WT pattern showing that paternal FAC1::GUS expression is detected both in the embryo and in the endosperm after fertilization. (C) Abnormal GUS expression pattern in a *tir1 afb1-1 afb2-2 afb3-3* embryo sac showing paternal FAC1::GUS expression in an embryo proper and in a proembryo arrested after the first zygotic division, and no endosperm development. From a total of 399 *tir1 afb1-1 afb2-2 afb3-3* embryo sacs examined, 82 showed defects in egg cell and synergid morphology while 26 aborted at FG1 stage. Ccn, central cell nucleus; EcL, egg cell-like; End, endosperm; Ep, embryo proper; PE, proembryo; Syn, synergid. Nuclei in panel (A) are artificially colored in red, and the proembryo in (C) and embryos in (B) and (C) are outlined by dotted lines. Bar indicates 20 μm.

Table S1. Expression of the synthetic reporter *DR5::GFP* in embryo sacs defective for *ARFs* expression. Pistils of *pES1::LhG4/+; Op::amiR-ARFa/+; DR5::GFP /+* plants were examined for *GFP* expression in the embryo sac.

Pistils studied	GFP expression		Total	P value *
	GFP positive	GFP negative		
Op::amiR-ARFa/+; pES1::LhG4; DR5::GFP/+	102 (32.07 %)	216 (67.92 %)	318 (100 %)	<0.005
pES1::LhG4/+; DR5::GFP/+	257 (51.19 %)	245 (48.81 %)	502 (100%)	>0.05

*χ2-Test from the expectation that 50 % of the gametophytes will be GFP positive as a result of *DR5::GFP* being expressed in the embryo sacs. A second χ2-Test was performed for the expectation that 37.5% of the gametophytes will be GFP positive as a result of *amiR-ARFa* being expressed in *DR5::GFP* embryo sacs, if the a*miR-ARFa* is fully penetrant. The P value obtained was >0.1, meaning that the deviation observed in the *Op::amiR-ARFa / +; pES1::LhG4 / +; DR5::GFP / +* pistils from the expected 37.5% for GFP positive embryo sacs is not statistically significant.

Table S2. . Embryo sac analysis in pistils from plants carrying the Op*::amiR-ARFa* construct crossed to plants with *LhG4* expression driven by the embryo sac promoter *pES1*. Ten independent transgenic plants carrying the *Op::amiR-ARFa* construct were crossed to plants with *LhG4* expression driven by the embryo sac promoter *pES1* and 30 F1 plants were studied. Eight F1 plants showed a strong phenotype, with a ratio of defective embryo sacs near 25%. In carpels of *pES1::LhG4*/+; *Op::amiR-ARFa/+* plants, 25% of the embryo sacs are predicted to inherit both constructs and result in the down-regulation of *ARF* expression.

.

Pistils studied	Phenotypes observed			Total	p value[*2]
	WT embryo sacs	Defects in micropylar cells polarity	Collapsed embryo sacs		
Op::amiR-ARFa / + *x* *pES1:: LhG4* / +	534 (77.84 %)	121 (17.64 %)	31 (4.52 %)[*1]	686 (100 %)	>0.05

[*1] The proportion of aborted embryo sacs is comparable to the one described for WT pistils.

[*2] $\chi 2$-Test from the expectation that 25% of the gametophytes will be defective as a result of *amiR-ARFa* expression in the embryo sacs.

Table S3. Expression of cell specific markers in embryo sacs defective for *ARF* expression. Pistils of *pES1*::LhG4/+; *Op::amiR-ARFa/+; GUS/+* plants were examined for GUS expression in the embryo sac.

Pistils studied	GUS positive WT expression pattern	GUS negative	GUS positive Abnormal expression pattern	Total	P values *
pES1>>amiR-ARFa x Egg cell marker line	189 (38.72 %)	289 (59.22 %)	10 (2.05 %)	489 (100 %)	$6.376\ e^{-07}$
pES1>>amiR-ARFa x Synergid cell marker line	97 (23.26 %)	320 (76.74 %)	0	417 (100 %)	$< 2.2\ e^{-16}$
pES1>>amiR-ARFa x Central cell marker line	185 (46.48 %)	213 (53.52 %)	0	398 (100 %)	0.1605
pES1>>amiR-ARFa x Antipodal cell marker line	220 (49.33 %)	226 (50.67 %)	0	446 (100 %)	0.7763

* χ2-Test from the expectation that 50% of the gametophytes will be GUS positive, WT expression pattern (i.e. express the cell-specific marker in the correct cells), due to segregation of the GUS reporter. Of the total embryo sacs, 25% are predicted to be defective for *ARF* expression, and 12.5% are predicted to be both defective for *ARF* expression and carrying the GUS reporter.

Table S4. Embryo sac analysis in pistils from plants carrying the *Op::YUC1* construct that were crossed to plants with *LhG4* expression driven by the embryo sac promoter *pES1*. Ten independent transgenic plants carrying the *Op::YUC1* construct were crossed to plants with *LhG4* expression driven by the embryo sac promoter *pES1* and 30 F1 plants were studied. Six F1 plants showed a strong phenotype, presenting a ratio of defective embryo sacs near 25%. In carpels of *pES1::LhG4*/+; *Op::YUC1* plants, 25% of the embryo sacs are predicted to inherit both constructs resulting in over-expression of *YUC1*.

Pistils studied	Phenotypes observed				Total	P value *
	WT	Defects in micropylar cells polarity	Unfused polar nuclei	Collapsed embryo sacs[a]		
pES1>>YUC1	376 (74.60)	64 (12.70 %)	5 (1.00 %)	59 (11.70 %)	504 (100 %)	>0.05

[a]In WT pistils, the frequency of collapsed embryo sacs is 4-5% (see Table S1).

* χ2-Test from the expectation that 25% of the gametophytes will be defective as a result of *YUC1* overexpression in the embryo sacs.

Table S5. Expression of cell specific markers in embryo sacs overexpressing *YUC1* of *pES1*::*LhG4/+; Op::YUC1/+; GUS/+* plants were examined for GUS expression in the embryo sac.

Pistils studied	GUS positive WT expression pattern	GUS negative	GUS positive Abnormal expression pattern			Total (100 %)	P values *
			Whole E. Sac	Central cell	Antipodal cells		
pES1>>YUC1 x Egg cell marker line	111 (21.94 %)	362 (71.54 %)	2 (0.40 %)	0	31 (6.13 %)	506 (100 %)	$< 2.2 e^{-16}$
pES1>>YUC1 x Synergide cell marker line	154 (29.61 %)	328 (63.07 %)	12 (2.30 %)	5 (0.96 %)	21 (4.04 %)	520 (100 %)	$< 2.2 e^{-16}$
pES1>>YUC1 x central cell marker line	260 (42.28 %)	355 (57.72 %)	0	0	0	615 (100 %)	0.0001277
pES1>>YUC1 x Antipodal cell marker line	118 (27.76 %)	307 (72.24 %)	0	0	0	425 (100 %)	$< 2.2 e^{-16}$

* χ2-Test from the expectation that 50% of the gametophytes will be GUS positive, WT expression pattern (i.e. express the cell-specific marker in the correct cells), due to segregation of the GUS reporter. Of the total embryo sacs, 25% are predicted to overexpress *YUC1*, and 12.5% are predicted to be both overexpressing *YUC1* and carrying the GUS reporter

Supplemental references

S1 C. M. Liu, D. W. Meinke, *Plant Journal* 16, 21 (1998).

S2 G. C. Pagnussat, H. J. Yu, V. Sundaresan, *Plant Cell* 19, 3578 (2007).

S3 J. P. Alvarez *et al.*, *Plant Cell* 18, 1134 (2006).

S4 A. Goldshmidt *et al.*, *Plant Cell* 20:1217-1230 (2008).

S5 S. J. Clough, A. F. Bent, *Plant Journal* 16, 735 (1998).

S6 H-J. Yu *et al*., *Plant Physiol*. 139, 1853-1869 (2005).

S7 Y. Okushima *et al., Plant Cell* 18, 1134 (2006).

S8 D. Wang *et al.*, *Gene* 394, 13–24 (2007).

S9 D. L. Remington *et al.*, *Plant Physiol*. 135, 1738–1752 (2004).

S10 A. C. Mallory, *et al.* , *EMBO J*., 23, 3356-3364 (2004).

S11 M. Schuetz *et al.*, *Plant Physiol*. 148, 870-880 (2008).

S12 J. Xu, *et al.*, Plant J. 42: 743–756 (2005).